Desalination and Water Treatment
www.deswater.com
doi: 10.5004/dwt.2018.23003

130 (2018) 17–27
October

Fouling of reverse osmosis membrane applied to membrane bioreactor effluent treating landfill leachate treatment under various pH conditions

Samunya Sanguanpak[a], Weerapong Rukapan[b], Wilai Chiemchaisri[b], Chart Chiemchaisri[b,*]

[a]*National Metal and Materials Technology Center (MTEC), National Science and Technology Development Agency (NSTDA), 114 Thailand Science Park, Paholyothin Rd., Klong Luang, Pathumthani 12120, Thailand, email: samunys@mtec.or.th*
[b]*Department of Environmental Engineering, Faculty of Engineering, Kasetsart University, Bangkok 10900, Thailand, emails: fengccc@ku.ac.th (C. Chiemchaisri), johnny_johnest@hotmail.com (W. Rukapan), fengwlc@ku.ac.th (W. Chiemchaisri)*

Received 19 March 2018; Accepted 25 August 2018

ABSTRACT

This research investigates the fouling behavior of reverse osmosis (RO) membranes in an integrated membrane bioreactor (MBR)-RO system for landfill leachate treatment. In a long-term operation under natural alkaline condition (pH 8.0–8.5), a full-scale integrated MBR-RO system achieved high treatment efficiencies (>95%) but suffered RO membrane fouling as a result of calcium scaling. Specifically, in the study, the mixed liquor pH in MBR was varied between 5.5, 6.5, 7.5, and 8.5, and the effect on RO membrane fouling examined in laboratory-scale experiments. The results showed that pH influenced the removal of dissolved organic matters in the MBR and the characteristics of MBR permeates. At pH 5.5, the deposition of protein-like substances substantially reduced the RO flux, and calcium scaling on the RO membrane was clearly visible under pH 8.5. The RO flux slightly decreased under pH 6.5 and 7.5. The optimal pH for treating landfill leachate using the integrated MBR-RO system was between 6.5 and 7.5.

Keywords: Calcium scaling; Landfill leachate; MBR; Mixed liquor pH; RO

1. Introduction

Landfill leachate is high strength wastewater that drains or leaches from landfills. It varies in composition in response to landfill age and waste type. According to Renou et al. (2008) [1], landfill leachate typically contains organic matters, ammonia, heavy metals, and toxic materials. In treating landfill leachate, existing biological treatment methods prove ineffective in remediation of leachate high in biodegradation-resistant organic substances. Thus, alternative treatment methods that combine the physicochemical and biological treatment techniques were proposed for improved treatment performance [1]. Of particular interest is the treatment system that integrates membrane bioreactor (MBR) with reverse osmosis (RO). The integrated MBR-RO technology is proven operationally and environmentally promising for landfill leachate treatment and reclamation [2–4].

However, in the integrated MBR-RO system, the fouling of RO membranes hampers wider adoption of this hybrid technology. According to Ke et al. [5], RO membrane fouling is subject to the characteristics of feed water. In MBR treatment, the biological and filtration mechanisms could remove most organic substances [6]; however, the microfiltration (MF) membranes sometimes failed to capture some soluble substances, resulting in the presence of total organic carbon (TOC) and extracellular polymeric substances (EPS) in the MBR permeate and the fouling propensity of RO membranes.

According to Jacob et al. [7], the MBR permeate with low TOC concentrations induced low RO membrane fouling vis-à-vis that with high TOC concentrations. In addition, the recirculation of RO concentrates to the MBR unit contributed to solids precipitation and inorganic fouling in

* Corresponding author.

RO/nanofilter (NF) membranes [8]. To mitigate the fouling in the RO system treating landfill leachate, pretreatments, including cartridge filters, activated carbon filters, addition of biocides, and antiscalants were used to improve the feed water quality [9].

In the integrated MBR-RO system, RO membrane fouling is also influenced by the MBR operating condition. Specifically, the MBR permeate characteristics are a function of the MBR operating condition, for example, the organic loading, food to microorganisms [10], and sludge retention time [11–12], which in turn affects the fouling propensity of the RO membrane. According to Wu et al. [13] and Tadkaew et al. [14], pH played an important role in the MBR performance. In fact, the effect of pH on the treatment efficiency was extensively researched. However, studies on the effect of different pH conditions in MBR on the RO membrane fouling behavior in an integrated membrane treatment system are very limited.

This research aims to investigate the performance of an integrated MBR-RO landfill leachate treatment system and RO membrane fouling behavior. In the study, the removal organic matters were determined. In addition, the RO membrane flux under four mixed liquor pH conditions (5.5, 6.5, 7.5, and 8.5) were determined and compared. This study is expected to shed light on the membrane fouling behavior during the treatment of landfill leachate using the integrated MBR-RO system, and thus offer a strategy to mitigate the membrane fouling through optimizing the mixed liquor pH in the MBR.

2. Materials and methods

2.1. Pilot-scale leachate treatment system

Fig. 1 illustrates the pilot-scale integrated MBR-RO landfill leachate treatment system, including an anoxic tank (3 m^3 working volume), an incline tube, an aerobic tank (3 m^3 working volume), and an RO unit with a treatment capacity of 6 $m^3 d^{-1}$. Inside the aerated MBR tank was two submerged membrane modules (0.4 μm polyvinylidene fluoride hollow-fiber membrane) for capturing suspended solids, and the dissolved oxygen (DO) concentrations were maintained at 3–4 mg L^{-1}. Total hydraulic retention time (HRT) was 1 d (12 h each for the anoxic unit and the MBR unit), and the system was operated without sludge wastage except for sampling purposes. Mixed liquor suspended solids (MLSS) concentrations were 8–12 g L^{-1} and the sludge recirculation to the anoxic tank was at 100% feed flow rate.

In leachate treatment, RO filtration is utilized as a post-treatment to improve overall removal efficiency of the system. In Fig. 1, the MBR-treated water (MBR permeate) was first fed through a cartridge filter (5 μm pore size) to sieve out particulates and transferred to the RO pressure vessel for removal of remaining dissolved organic and inorganic contaminants. The RO vessel was of cross-flow-cell rectangular stainless steel embedded with three spiral wound elements (i.e., two running elements and one standby element).

In this pilot-scale system, low-fouling aromatic polyamides composite RO membranes with an active area of 8 m^2 (TML10F, TORAY Industrial Inc.) were used in the RO treatment. The RO unit was operable with a 50% recovery, and the operating pressure was 0.5–1.5 MPa. To minimize membrane fouling, biocide (Kuriverter® IK-110) and an antiscalant (Kuriverter® N-500) of 5 mg L^{-1} each were fed continuously into the system. In addition, the RO membranes were either cleaned-in-place once a month or when the operating pressure reached the upper limit of 1.5 MPa, using sodium hydroxide (NaOH) and citric acid. The RO-treated water (RO permeate) was for nonpotable purposes, and the RO concentrates were used as fertilizers and recirculated to the MBR.

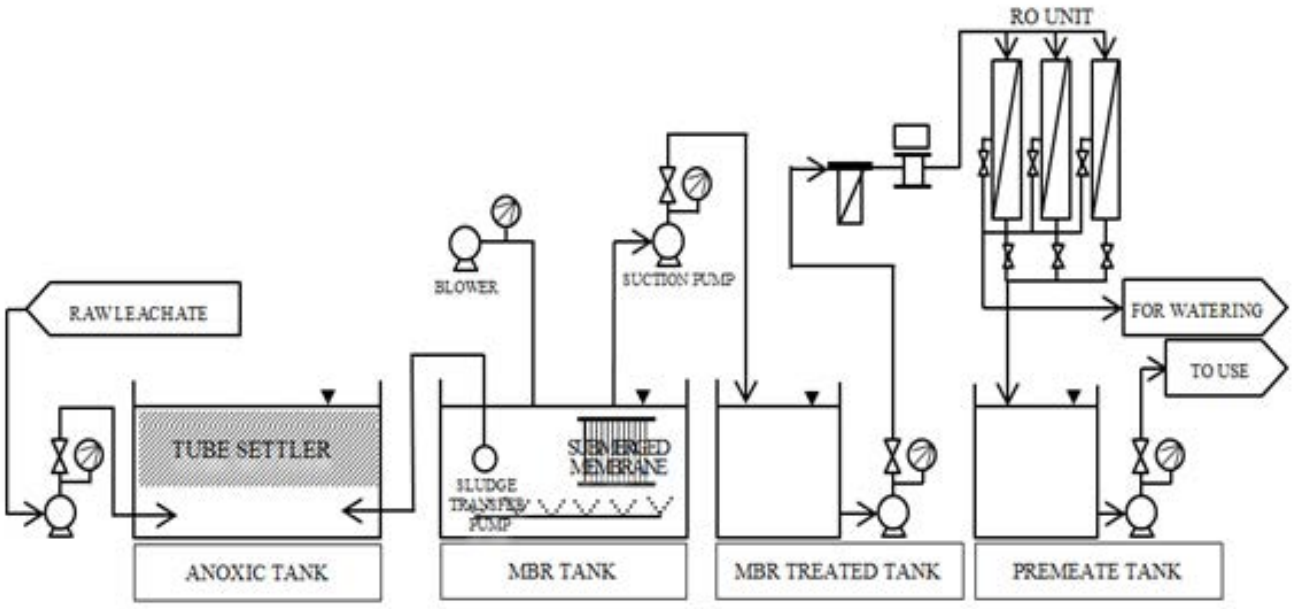

Fig. 1. Schematic of the integrated MBR-RO system.

2.2. Laboratory-scale MBR-RO experimental unit

2.2.1. MBR setup and operating condition

Fig. 2(a) illustrates the schematic of the experimental MBR consisting of two 12-L lab-scale MBR tanks (MBRs 1 and 2), each outfitted with submerged hollow-fiber membrane module (0.4 μm PVDF with 0.07 m^2 surface area). To maintain the DO concentration at 3–4 mg L^{-1}, air pumps were deployed for a continual supply of aeration. The HRT in the reactor was 1.5 d and the permeate flux was maintained at 4.5 L m^{-2} h^{-1}. Prior to the MBR treatment, influent was prepared by diluting fresh leachate from a solid waste disposal site with tap water at 1:10 (v/v) to maintain the organic loading at 3.7 ± 0.5 kg m^{-3} d^{-1} for BOD and 5.4 ± 0.9 kg m^{-3} d^{-1} for COD. The MLSS concentrations were 10–15 g L^{-1}. Furthermore, in MBR 1, the mixed liquor pH was varied from its natural pH condition (8.0–8.5) to 6.5 ± 0.3 during the first phase (days 1–75) and then 5.5 ± 0.3 during the second phase (days 76–150). Meanwhile, in MBR 2, the mixed liquor pH was first elevated to 8.5 ± 0.2 and then reduced to 7.5 ± 0.1 in the first and second phases of the operation. The pH adjustments were carried out using analytical grade HCl (1 M) and NaOH (1 M) solutions. The mixed liquor pH was measured on an hourly basis using digital pH meter. After 60 d (the steady condition), the MBR permeates under different pH conditions were fed into the RO filtration unit.

2.2.2. RO filtration experiment and operating condition

In Fig. 2(b), the MBR permeate was first fed into the stainless steel lab-scale membrane filtration unit using a high pressure pump inside a controlled-temperature room (25°C). A by-pass valve was used to regulate the operating pressure and permeate flow rate. In this research, fouling on the RO membrane was characterized following the cleaning protocol in Rukapan et al. [9]. Specifically, the fouled membrane was first removed from the filtration vessel and cut into smaller sheets with a surface area of 9.62 cm^2. The cut membranes were then subjected to sequential cleaning by pure water, NaOH (pH~12), and citric acid (pH~2) at the cross-flow velocity of 0.15 m s^{-1} for 30 min, and the extent of fouling and type of foulant subsequently evaluated.

In addition, the effect of mixed liquor pH on the RO membrane fouling behavior was investigated whereby the low-fouling composite polyamide RO flat sheet membranes with high hydrophilicity and neutrally charged surface (LFC3-LD, Nitto Denko) were cut into small pieces of 9.62 cm^2 in surface area. The cut membranes were then equilibrated with deionized water to allow for sufficient membrane compaction. The MBR permeate under different mixed liquor pH conditions was fed into the filtration unit using high pressure pump. The feed flow rate and cross-flow velocity were 10 mL $min^{-1}$and 0.15 m s^{-1}, respectively. In addition, the filtration pressure was maintained at 1.0 ± 0.1 MPa. The RO permeate volume was measured every 30 min over 10 h filtration period and excess concentrated water recycled.

2.3. Analytical methods

2.3.1. Analysis of leachate and permeate

The electrical conductivity (EC) and pH were measured using EC and pH meters. The suspended solids (SS), total dissolved solids (TDS), biochemical oxygen demand (BOD_5),

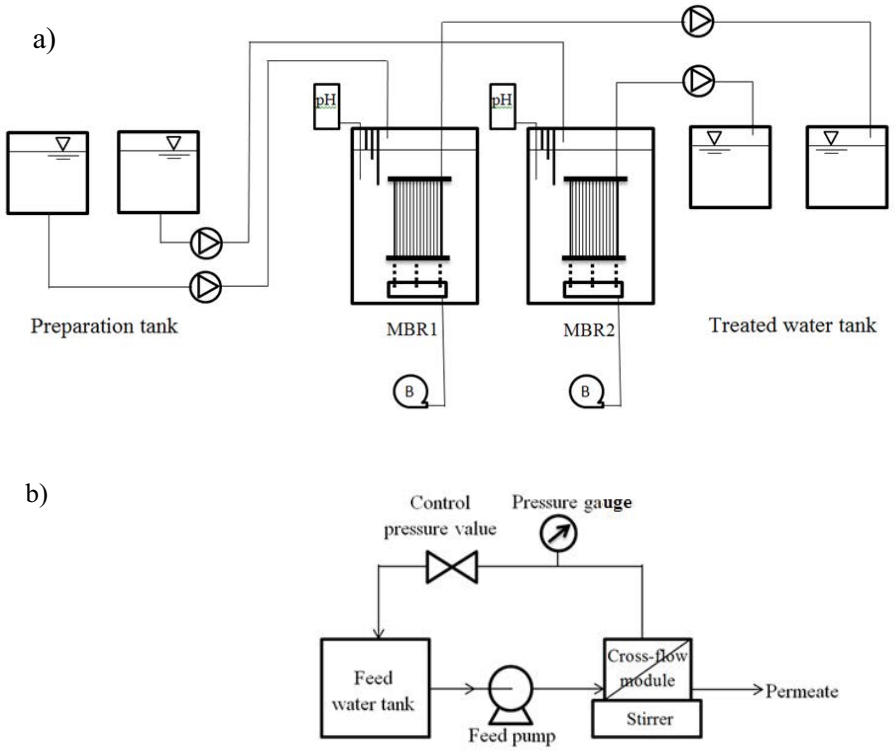

Fig. 2. Schematic of (a) MBR, and (b) RO experimental system.

chemical oxygen demand (COD), and alkalinity were determined in accordance with the standard methods (APHA, 2005) without pretreatment.

The dissolved organic matters (DOM) were prepared by dilution and filtered with 0.45 μm membrane filter. The dissolved organic carbon (DOC) and UV_{254} were respectively determined by Shimadzu TOC-5000 TOC and Thermo Scientific™ evolution 60S spectrophotometer. The specific UV absorbance ($SUVA_{254}$) was calculated by dividing UV_{254} by DOC. The ion concentrations of calcium and magnesium were quantified using Shimadzu HIC-10A ion chromatograph. EPS were determined by total carbohydrates and proteins, whereby proteins were colorimetrically determined by folin method with bovine serum albumin (BSA) as the standard and carbohydrates by phenol-sulfuric acid with glucose as the standard. Fluorescence excitation-emission matrix (EEM) spectroscopy was carried out using Jasco FP-8200 spectrofluorometer with 1 cm quartz cell.

Prior to analysis, the water samples were diluted to a DOC concentration of 10 mg L^{-1}. The EEM spectra were collected at the excitation (Ex) and emission (Em) wavelengths of 200–500 nm and 250–600 nm with 5 nm increment. The spectra were scanned with 5 nm slit bandwidth at a scan rate of 2,000 nm min^{-1}. The spectrum of deionized (DI) water was recorded as blank and the equipment autozeroed. The measurements were carried out in triplicate in a controlled-temperature room (25°C).

2.3.2. Membrane fouling

In this research, membrane fouling was categorized into particulate fouling removable by water, organic fouling by NaOH, and inorganic fouling by citric acid. The permeate flux and membrane resistance can be respectively calculated by Eqs. (1) and (2):

$$J = \frac{dV}{dtA} = \frac{\left(\Delta P - \Delta\pi\right)}{\eta\left(R_m + R_f\right)} \tag{1}$$

where J is the permeate flux ($m^{-1}\ h^{-1}$), V is the collected volume, A is the membrane surface area, and t is time. ΔP is the pressure difference between the feed and permeate sides (MPa), $\Delta\pi$ is the osmotic pressure difference between the feed and permeate sides (MPa), and η is the dynamic viscosity (Pa.s). The membrane resistance (R_m, m^{-1}) can be estimated from the initial water flux (J_{wi}) as

$$R_m = \frac{\left(\Delta P - \Delta\pi\right)}{\eta\Sigma J_{wi}} \tag{2}$$

The resistance due to fouling (R_f, m^{-1}), which is a function of time and operating condition, can be calculated from the water flux after the sequential cleaning (J_{wc}):

$$R_f = \left(\frac{\left(\Delta P - \Delta\pi\right)}{\eta\Sigma J_{wc}}\right) - R_m \tag{3}$$

The membrane surface morphology and elemental composition were characterized by JEOL JSM-5410 scanning electron microscope with energy dispersive spectrometer (SEM/EDS). The fouled and cleaned membranes were rinsed with distilled water and dried at room temperature prior to surface characterization. The functional groups on the membrane samples were determined by Perkin–Elmer spectrum spotlight Fourier-transform infrared (FTIR) imaging system using Micro-ATR technique. The FTIR spectra were examined under the middle wavelength infrared of 4,000–600 cm^{-1}.

3. Results and discussion

3.1. Removal performance of the MBR-RO system

Table 1 tabulates the characteristics of the influent, MBR, and RO permeates relative to the standards of Thailand's Ministry of Industry. The leachate influent was relatively acidic (pH 4.74–5.17) with high concentrations of ionic constituents: 4,080 mg L^{-1} TDS, 432 mg L^{-1} Ca, and 213 mg L^{-1} Mg.

Table 1
Characteristics of influent and treated leachate of the integrated MBR-RO system

Parameter	Influent	MBR permeate	RO permeate	Standard[a]
pH	5.17 ± 0.43	8.28 ± 0.37	7.51 ± 0.42	5.5–9.0
SS (mg L^{-1})	644 ± 120	2 ± 1	0	–
TDS (mg L^{-1})	4,080 ± 210	3,342 ± 352	147 ± 76	3,000
COD (mg L^{-1})	9,850 ± 890	820 ± 86	31 ± 25	120
BOD (mg L^{-1})	6,440 ± 460	150 ± 11	10 ± 8	20
DOC (mg L^{-1})	5,294 ± 410	215 ± 25	8 ± 5	–
TKN (mg L^{-1})	255 ± 140	39 ± 13	6 ± 4	100
UV_{254} (cm^{-1})	11.96 ± 0.85	5.84 ± 0.88	0.06 ± 0.03	–
$SUVA_{254}$(L mg^{-1} m^{-1})	0.23 ± 0.03	2.72 ± 0.14	0.75 ± 0.10	–
Alkalinity (mg L^{-1} as $CaCO_3$)	3,060 ± 350	1,989 ± 150	91 ± 27	–
Ca (mg L^{-1})	432 ± 44	234 ± 41	5 ± 4	–
Mg (mg L^{-1})	213 ± 38	216 ± 23	3 ± 2	–

[a]Industrial effluent standard, Ministry of Industry, Thailand.
No. of samples = 5.

It also exhibited several biodegradation characteristics [1] with average COD, BOD, and DOC of 9,850 mg L^{-1}, 6,440 mg L^{-1}, and 5,294 mg L^{-1}, respectively.

Following the MBR treatment, the permeate pH rose to 7.9–8.7 probably due to considerable amounts of CO_2 being removed by air sparging in the aerated MBR tank. COD, BOD, and TOC were efficiently degraded by 92%, 98%, and 96%. Nevertheless, the $SUVA_{254}$ of aromatic organic compounds, that is, humic substances, increased from 0.23 (influent) to 2.72 L $mg^{-1}m^{-1}$ indicated that the MBR was effective in the removal of nonaromatic compounds but ineffective degrading recalcitrant organic compounds, for example, humic substances.

For total organic nitrogen and ammonia nitrogen, the TKN removal was 78%–96%. The concentrations of ion constituents (TDS, Ca, and Mg) were reduced by 10%–50% through chemical precipitation and/or biomass adsorption. Consistent with Sanguanpak et al. [6] and Chiemchaisri et al. [15], the MBR process of this research could achieve high treatment efficiencies through the removal of biodegradable organic matters, while the refractory organic compounds and dissolved ion constitutes could partially be removed and were thus present in the MBR permeate.

To address, the MBR permeate was further treated with the RO membrane unit whereby most of the remaining contaminants were captured and removed. The RO permeate (i.e., final effluent) possessed the characteristics that meet the water standards for nonpotable purposes. In essence, the integrated MBR-RO system could remove more than 99%, 97%, and 96% of organic matters, TKN, and ion.

3.2. Fouling characteristics of the RO membrane

In this research, the RO membrane fouling behavior was characterized and a strategy to mitigate the fouling in the RO unit identified. Specifically, the system was operated under a permeate flux of 15.6 L m^{-2} h^{-1} with 50% recovery. However, once the operating pressure reached 1.5 MPa (in approximately 20 d), the membranes were cleaned-in-place with NaOH and citric acid. At termination (approximately 1 year later), the fouled RO membranes were removed from the vessels and their characteristics determined. Pure water, alkaline (NaOH), and acid solutions (citric acid) were used as the cleaning agents to remove the particulate matters, organic foulants, and inorganic scaling from the membrane surface and pores.

Table 2 tabulates the filtration resistance and normalized flux of the fouled and cleaned membranes. The sequential cleaning could achieve the resistance removals of 22.29% with pure water, 32.01% with NaOH, and another 37.41% with citric acid, along with increase in the normalized flux from 44.26% (fouled membrane) to 74.60%. By comparison, citric acid was most effective in removing the foulants, indicating that inorganic scaling was the most abundant fraction of accumulated foulants. In contrast, according to Rukapan et al. [9], NaOH was the most effective cleaning agent to remove the foulants from the RO membranes in full-scale leachate treatment. In fact, in [9], the leachate influent was pretreated with chemical coagulation and sand filtration, resulting in the discrepancy in the effective chemical agents for membrane cleaning.

Table 2
Resistance and normalized flux of fouled and cleaned RO membranes

Membrane sample	Filtration resistance (10^{14} m^{-1})	Resistance removal (%)	Normalized flux (%)
Fouled membrane	2.06		44.26
Cleaned membrane			
After water cleaning	1.60	22.29	49.48
After NaOH cleaning	0.94	32.01	58.36
After citric cleaning	0.17	37.41	74.60

Note: Membrane fouling can be categorized into particulate fouling, organic fouling, and inorganic fouling that can be removed by pure water, NaOH, and citric acid, respectively.

Fig. 3 illustrates the SEM images and elemental composition of the fouled and cleaned membranes. A layer of foulant was visible on the fouled membrane surface, while more and more of the deposited particulates were removed by pure water, NaOH, and citric acid. The EDS elemental analysis indicated that the foulant was made up of C, O, Mg, Ca, Al, Si, and Fe, with Ca the dominant element on the fouled membrane surface. Following the sequential cleaning, Ca declined while C (representing the membrane surface) became dominant. However, some residual inorganic elements (Al, Ca, and Fe) remained, indicating irreversible fouling. Ruan et al. used the same type of RO membrane in a pilot-scale hybrid membrane process to treat biogas slurry and reported that the inorganic deposits ($CaCO_3$, $Mg(OH)_2$, and $CaSO_4$) and complex organic matters (hydrocarbon and aliphatic acid) were dominant in the foulants on the RO membrane surface. In addition, most inorganic fouling could be removed by HCl solution, while NaOH was effective in removing the organic foulants [16].

Fig. 4 illustrates the FTIR spectra of the fouled and cleaned RO membranes. The absorption bands of the fouled membrane were 1,650 and 1,540 cm^{-1} corresponding to amides I (C=O stretching) and II (N-H in plane). A peak was observed around 1,425 cm^{-1}, which could be attributed to the symmetrical stretches of –COO– of amino acids [17]. Furthermore, other peaks at 2,528, 880, and 718 cm^{-1} were observed, corresponding to the asymmetric and symmetric CO_3 deformation, while the peaks at 1,425 and 1,810 cm^{-1} were characteristic of symmetric CO_3 stretching and CO_3 deformation [18]. The finding suggested the presence of proteins and inorganic carbonate in the foulant.

However, the FTIR spectra of the water- and NaOH-cleaned membranes were similar to the fouled membrane. This could be attributed to an abundance of inorganic precipitates and/or biological precipitation of inorganic-organic complexes formed on the membrane surface [19]. After the cleaning with citric acid, the peaks of inorganic carbonate mostly disappeared while the strong absorption bands of the original aromatic polyamide membrane at 1,780, 1,720, and 1,378 cm^{-1} could be observed [20], representing imide functional groups. This suggested that calcium carbonate ($CaCO_3$) was the dominant foulant on the RO membrane surface in the MBR-RO system. In fact, $CaCO_3$ is a frequently

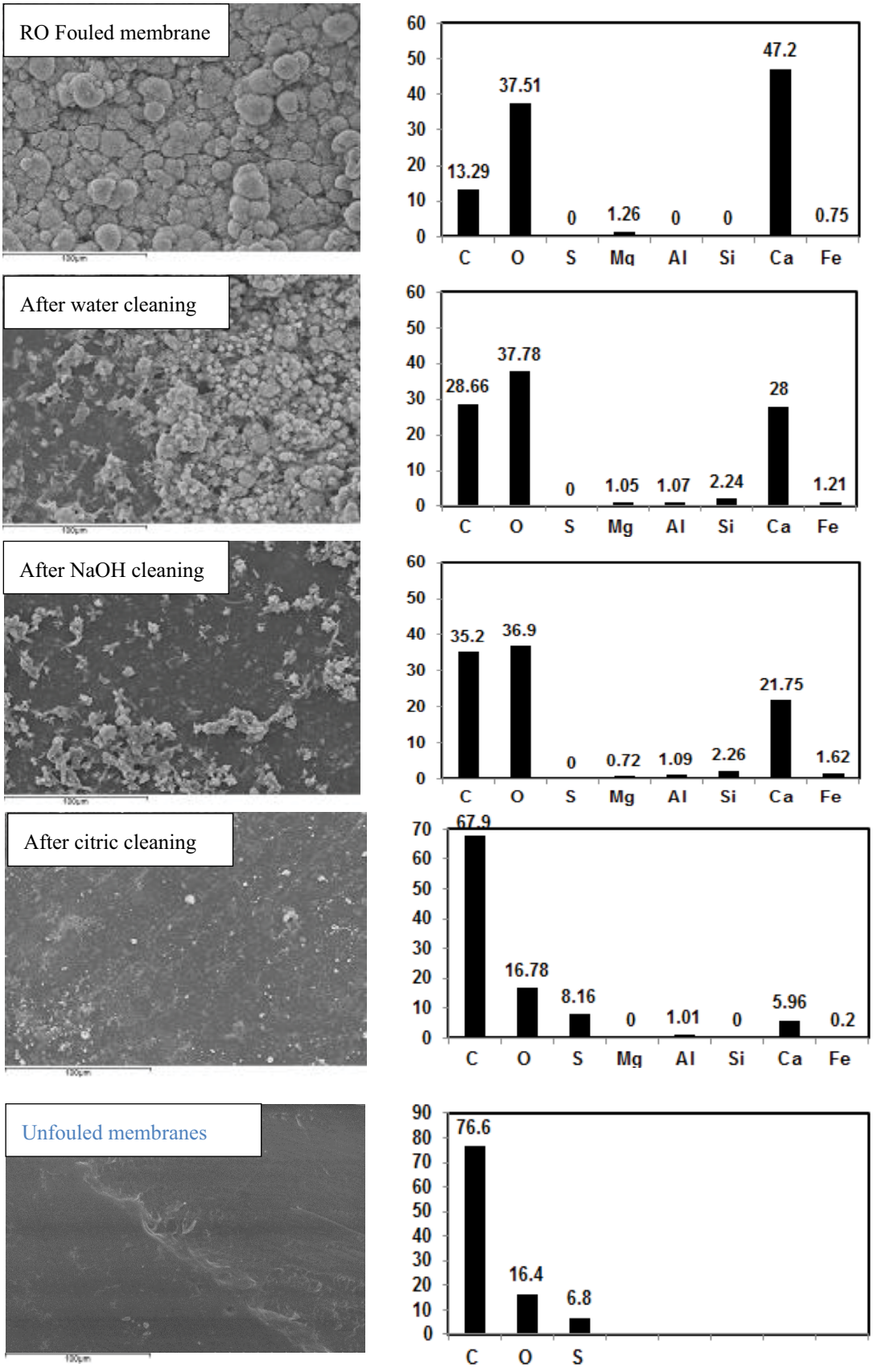

Fig. 3. SEM/EDX micrographs of fouled, cleaned, and unfouled RO membranes (×500 magnification).

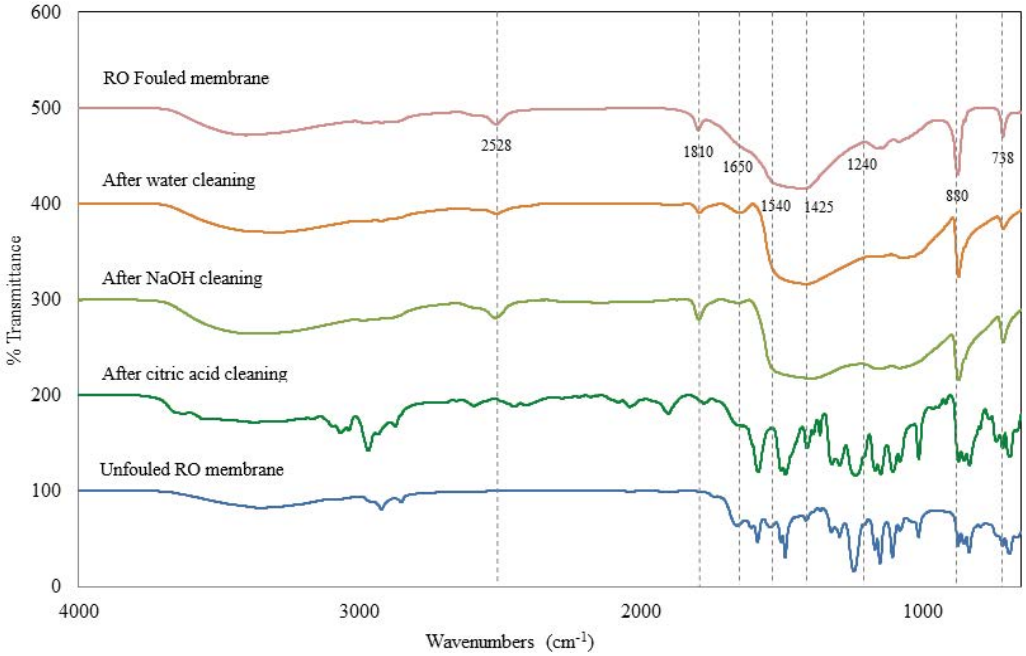

Fig. 4. FTIR spectra of fouled, cleaned, and unfouled RO membranes.

encountered scale on the RO membrane, especially in brackish water desalination plants [21]. In this study, the Langelier Saturation Index (LSI) of MBR permeate was 2.2. According to Antony et al. [22], a large positive LSI indicates severe $CaCO_3$ precipitation and scaling [22].

3.3. Effect of mixed liquor pH on MBR permeate characteristics

The physicochemical properties of MBR permeate and RO membrane fouling were determined by varying the mixed liquor pH in the MBR tanks (MBRs 1 and 2) between 5.5, 6.5, 7.5, and 8.5. Both MBRs were operated for 150 d. To maintain the comparable organic loading in the treated leachate from the anoxic tank in the pilot-scale MBR, fresh leachate was diluted with tap water (1:10) prior to the laboratory-scale MBR treatment. Table 3 tabulates the characteristics of the influent and MBR permeates under four pH conditions.

At pH 6.5, 7.5, and 8.5, the DOC concentrations were between 25 and 30 mg L^{-1}, achieving the removal efficiency of 97% on average. On the other hand, at pH 5.5, the DOC removal efficiency decreased. The lower removal efficiency in the pH 5.5 environment was attributable to the complex micro-organic changes in the MBR tanks. Specifically, certain species of micro-organisms became inactive [23], affecting degradation mechanism, and resulting in lower treatment performance.

According to Comstock et al. [24], higher $SUVA_{254}$ in the biological treatment process indicated high content of aromatic organic carbon and DOM removal efficiency by microbial activities. In Table 3, $SUVA_{254}$ increased to 1.17–2.96 cm^{-1} following the MBR treatment, indicating the biodegradability of nonaromatics in the MBR tanks. By comparison, $SUVA_{254}$ of the pH 5.5 MBR permeate was lowest, suggesting that the DOM removal efficiency declined as the mixed liquor pH decreased. In addition, the concentrations of proteins and carbohydrates in the pH 5.5 MBR permeate were highest.

Table 3
Characteristics of influent and MBR permeate as a function of operating pH

Parameter	Influent	Permeate at pH = 5.5	Permeate at pH = 6.5	Permeate at pH = 7.5	Permeate at pH = 8.5
pH	5.47 ± 1.0	5.66 ± 0.3	6.61 ± 0.23	7.96 ± 0.1	8.79 ± 0.06
DOC (mg L^{-1})	1,154 ± 205	68 ± 2	26 ± 10	25 ± 2	30 ± 2
UV_{254} (cm^{-1})	4.11 ± 0.09	0.79 ± 0.10	0.74 ± 0.12	0.74 ± 0.05	0.85 ± 0.05
$SUVA_{254}$ (L mg^{-1} m^{-1})	0.35 ± 0.06	1.17 ± 0.04	2.88 ± 0.03	2.96 ± 0.01	2.84 ± 0.02
Protein (mg L^{-1})	–	35 ± 3	21 ± 4	18 ± 3	24 ± 5
Carbohydrate (mg L^{-1})	–	11 ± 1	6 ± 1	5 ± 1	5 + 1
Calcium (mg L^{-1})	410 ± 105	392 ± 27	354 ± 33	164 ± 17	106 ± 12
Magnesium (mg L^{-1})	195 ± 35	193 ± 14	171 ± 18	136 ± 11	69 ± 9

No. of samples = 5.
Note: The samples were collected after 60 d and the effect of pH on MBR permeate qualities determined.

Specifically, the pH adjustment in the MBR tanks influenced the production of SMP and EPS, as well as residual proteins and carbohydrates in the permeate.

According to Gao et al. [25], proteins and carbohydrates in EPS could be affected by pH shocks, and the inorganic removal efficiency increased with increasing pH. Specifically, the inorganic removal efficiencies of Ca and Mg were 1%–4%, 12%–14%, 30%–60%, and 68%–74% for the mixed liquor pH of 5.5, 6.5, 7.5, and 8.5, respectively, suggesting a positive correlation between the inorganic removal and mixed liquor pH. Higher inorganic removal efficiency under elevated mixed liquor pH was attributable to the increased precipitation of Ca and Mg in the MBR tanks. Thus, varying the mixed liquor pH affected the MBR permeate characteristics. More specifically, at pH 5.5, the MBR permeate contained the highest DOC, proteins, carbohydrates, and inorganics.

In addition, the fluorescence properties of DOM under the four experimental pH conditions were analyzed. The MBR permeate samples were diluted to a DOC concentration of 10 mg L^{-1} prior to analysis. In Fig. 5, the analysis identified four fluorescence peaks, consistent with Comstock et al. [24] and Lu et al. [26]. In the figure, the fluorescence peaks at Ex/Em = 230–240/330–340 (peak A) and 270–290/300–340 (peak B) indicated aromatic protein-like and tryptophan protein-like substances, respectively. Peaks C and D at Ex/Em = 315–355/395–425 and 245–260/435–480 represented fulvic-acid-like and humic-like substances. At pH 5.5, the MBR permeate consisted of both protein-like substances (peaks A and B) and humic-like substances (peaks C and D). As the pH increased, the fluorescence peaks of humic-like substances (peaks C and D) were slightly red-shifted along the excitation and emission axes, while the fluorescence peaks of protein-like substances (peaks A and B) were blue-shifted.

A red shift is associated with an increase in aromatic poly-condensation and a higher degree of humification [27], suggesting higher humification in the MBR process, particularly under alkaline mixed liquor conditions. On the other hand, a blue shift is associated with a decomposition of condensed aromatic moieties and the break-up of large molecules into smaller fragments. Specifically, the differences in the EEM fluorescence spectra demonstrated the effect of varied mixed liquor pH on the organic structures and composition in the MBR permeates.

3.4. Effect of mixed liquor pH on RO membrane fouling

According to Ahn et al. [2], RO membrane technology was a post-treatment to remove residual dissolved organic pollutants, inorganic matters, and nonbiodegradable organic matters in the MBR-treated water. As previously discussed, the mixed liquor pH affected the physicochemical characteristics of MBR permeates and subsequent RO membrane fouling behavior. To verify, this research experimented with a lab-scale RO filtration unit and the RO concentrates were recycled.

Fig. 6 compares the normalized RO specific flux under different pH feed conditions and the effects of mixed liquor pH on the RO membrane fouling were assessed. In general, the RO membrane fouling behavior is a function of the MBR permeate, DOC, proteins, carbohydrates, Ca, and Mg. At pH 5.5, the rate of normalized specific flux decline was severest (65%) relative to the initial permeate flux, followed by at pH 8.5 (72%). Meanwhile, slight decrease in the flux (81%–83%) relative to the initial permeate flux was observed at pH 6.5 and 7.5.

According to Tang et al. [28], pH played an important role in RO/NF membrane fouling. At low pH, the flux decline was noticeable, possibly due to the increased adsorption of compounds on the membrane surface. On the other hand, at high pH, the dissociation between the functional groups of compounds and membrane surface increased, resulting in less fouling.

In this research, increased RO membrane fouling under the acidic and alkaline conditions (pH 5.5 and 8.5) could be attributed to the following reasons: (1) at pH 5.5, the MBR permeate was abundant with soluble organic

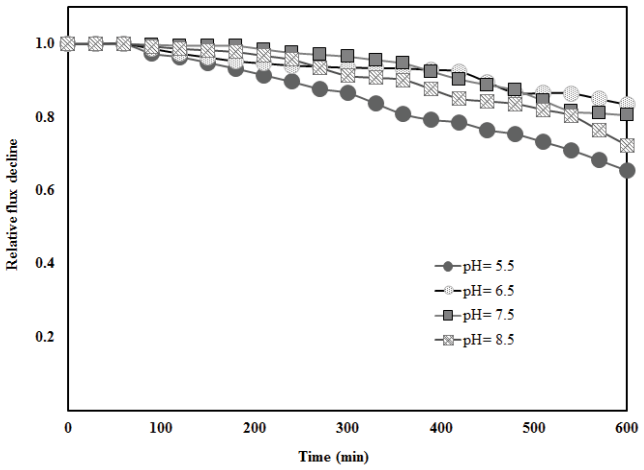

Fig. 6. Normalized specific flux of RO membrane as a function of operating pH.

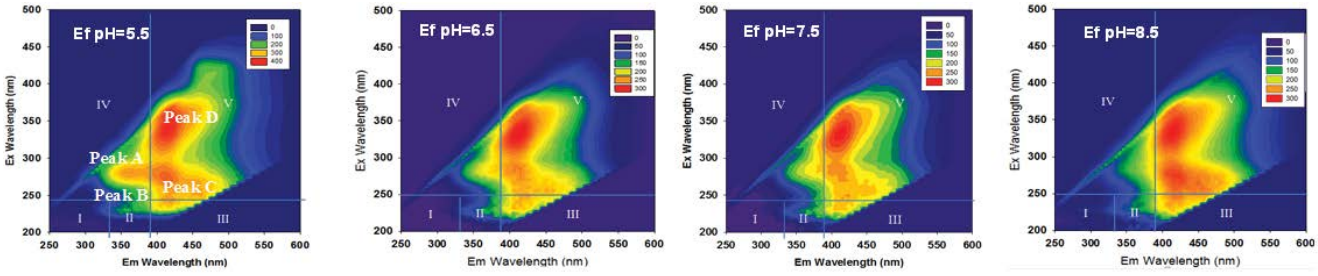

Fig. 5. Fluorescence EEM spectra of the MBR permeates at different operating pH.

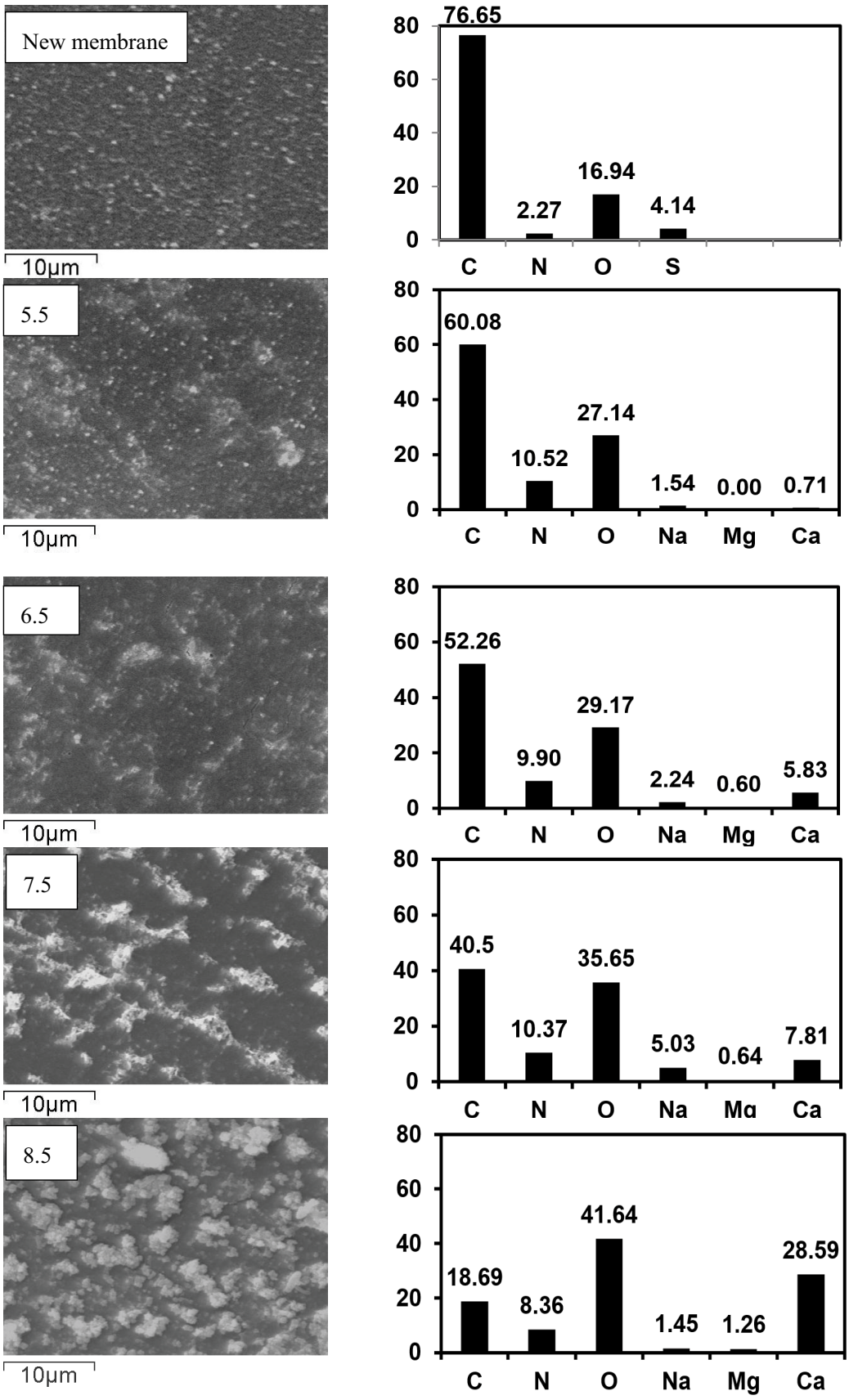

Fig. 7. SEM/EDX micrographs of new and fouled RO membranes under different pH of MBR permeate (3,500× magnification).

substances, including DOC, proteins, and carbohydrates. The compounds became less negatively charged at the low pH due to the reduced ionization of functional groups, such as carboxylic and phenolic. The phenomenon increased the deposition/adsorption of the compounds on the membrane surface and/or in the membrane pores, leading to more membrane fouling; and (2) at pH 8.5, the MBR permeate was high in humic-like substances. The humic substances interact with calcium ions, reducing the negatively charged groups and forming calcium bridges. These complex compounds increased precipitation and promoted membrane fouling.

Fig. 7 compares the scanning electron microscopy with energy dispersive X-ray spectroscopy (SEM/EDX) micrographs of a new and the fouled RO membranes under four pH conditions. At pH 5.5, a layer of smooth gel was formed on the membrane surface, while, at pH 8.5, a layer of precipitated foulant was visible. By visual inspection, biofouling was insignificant and thus the extent of biofouling was not quantified in this study. The energy dispersive spectroscopy (EDS) elemental analysis indicated the presence of C, N, O, Ca, Na, and Mg, with C, O, and N the dominant elements in the membrane fouling at pH 5.5, indicating that the organic substances, for example, proteins and polysaccharide, were the main foulants. On the other hand, Ca played a significant role in the membrane fouling under pH 8.5 condition, and the divalent cations of Ca could bridge with C, N, and O to form a dense fouling layer. The results showed that the RO membrane fouling was pH-dependent in that a dense gel layer of organic substances was formed at pH 5.5; and, at pH 8.0, the deposition of complex inorganic scaling substantially increased and worsened the RO flux.

4. Conclusions

This research is concerned with an integrated MBR-RO system for treating landfill leachate. In a long-term operation (>300 d), the integrated system could achieve more than 95% removal efficiencies of the pollutants. However, under leachate's natural alkaline condition (pH 8.0–8.5), the treatment system was fraught with calcium scaling on the RO membrane. To mitigate, pH in the MBR tanks was varied between 5.5, 6.5, 7.5, and 8.5. The findings showed that pH influenced the MBR permeate characteristics and subsequent RO membrane fouling behavior. The RO membrane fouling was severest under pH 5.5 due to the deposition of protein-like organic foulants. On the other hand, under pH 8.5, the calcium precipitation played a significant role in the RO membrane fouling. Essentially, the optimal pH for the integrated MBR-RO system was between 6.5 and 7.5.

Acknowledgments

This research was carried out under the Research and Development for Water Reuse Technology in Tropical Regions (WaterIntro) project of the Japan International Cooperation Agency (JICA) and the Japan Science and Technology Agency (JST). The authors would also like to extend deep gratitude to the Kasetsart University Research and Development Institute (KURDI) for financial support.

References

[1] S. Renou, J.G. Givaudan, S. Poulain, F. Dirassouyan, P. Moulin, Landfill leachate treatment: review and opportunity, J. Hazard. Mater., 150 (2008) 468–493.
[2] W.Y. Ahn, M.S. Kang, S.K. Yim, K.H. Choi, Advanced landfill leachate treatment using an integrated membrane process, Desalination, 149 (2002) 109–114.
[3] J. Chung, J.O. Kim, Wastewater treatment using membrane bioreactor and reverse osmosis process, Desal. Wat. Treat., 51 (2013) 5298–5306.
[4] M.C.S. Amaral, W.G. Moravia, L.C. Lange, M.M.Z. Roberto, N.C. Magalhães, T.L. dos Santos, Nanofiltration as post-treatment of MBR treating landfill leachate, Desal. Wat. Treat., 53 (2015) 1482–1491.
[5] X. Ke, R. Hongqiang, D. Lili, G. Jinju, Z. Tingting, A review of membrane fouling in municipal secondary effluent reclamation, Environ. Sci. Pollut. Res., 20 (2013) 771–777.
[6] S. Sanguanpak, C. Chiemchaisri, W. Chiemchaisri, K. Yamamoto, Removal and transformation of dissolved organic matter (DOM) during the treatment of partially stabilized leachate in membrane bioreactor, Water Sci. Technol., 68 (2013) 1091–1099.
[7] M. Jacob, C. Guigui, C. Cabassud, H. Darras, G. Lavison, L. Moulin, Performances of RO and NF processes for wastewater reuse: tertiary treatment after a conventional activated sludge or a membrane bioreactor, Desalination, 250 (2010) 833–839.
[8] C. Kappel, A.J.B. Kemperman, H. Temmink, A. Zwijnenburg, H.H.M. Rijnaarts, K. Nijmeijer, Impacts of NF concentrate recirculation on membrane performance in an integrated MBR and NF membrane process for wastewater treatment, J. Membr. Sci., 453 (2014) 359–368.
[9] W. Rukapan, B. Khananthai, C. Chiemchaisri, W. Chiemchaisri, T. Srisukphun, Short and long term fouling characteristics of reverse osmosis membrane at full scale leachate treatment plant, Water Sci. Technol., 65 (2011) 127–134.
[10] B. Wu, T. Kitade, T.H. Chong, T. Uemura, A.G. Fane, Impact of membrane bioreactor operating conditions on fouling behavior of reverse osmosis membranes in MBR–RO processes, Desalination, 311 (2013) 37–45.
[11] E.L. Farias, K.J. Howe, B.M. Thomson, Spatial and temporal evolution of organic foulant layers on reverse osmosis membranes in wastewater reuse applications, Water Res., 58 (2014) 102–110.
[12] E.L. Farias, K.J. Howe, B.M. Thomson, Effect of membrane bioreactor solids retention time on reverse osmosis membrane fouling for wastewater reuse, Water Res., 49 (2014) 53–61.
[13] J. Wu, Y. Zhuang, H. Li, X. Huang, pH adjusting to reduce fouling propensity of activated sludge mixed liquor in membrane bioreactor, Sep. Sci. Technol., 45 (2010) 890–895.
[14] N. Tadkaew, I.H. Faisal, J.A. Mcdonald, S.J. Khan, L.D. Nghiem, Removal of trace organics by MBR treatment: the role of molecular properties, Water Res., 45 (2011) 2439–2451.
[15] C. Chiemchaisri, W. Chiemchaisri, P. Nindee, C.Y. Chang, K. Yamamoto, Treatment performance and microbial characteristics in two-stage membrane bioreactor applied to partially stabilized leachate, Water Sci. Technol., 64 (2011) 1064–1072.
[16] H. Ruan, Z. Yang, J. Lin, J. Shen, J. Ji, C. Gao, B. Van der Bruggen, Biogas slurry concentration hybrid membrane process: Pilot-testing and RO membrane cleaning, Desalination, 368 (2015) 171–180.
[17] F. Meng, B. Liao, S. Liang, F. Yang, H. Zhang, L. Song, Morphological visualization, componential characterization and microbiological identification of membrane fouling in membrane bioreactor (MBRs), J. Membr. Sci., 361 (2010) 1–14.
[18] S. Gunasekaran, G. Anbalagan, S. Pandi, Raman and infrared spectra of carbonates of calcite structure, J. Raman Spectrosc., 37 (2006) 892–899.
[19] F. Meng, S.R. Chae, A. Drews, M. Kraume, H.S. Shin, F. Yang, Recent advances in membrane bioreactors (MBRs): membrane fouling and membrane material, Water Res., 43 (2009) 1489–1512.

[20] D. Wu, X. Liu, S. Yu, M. Liu, C. Gao, Modification of aromatic polyamide thin-film composite reverse osmosis membranes by surface coating of thermo-responsive copolymers P(NIPAM-co-Am). I: preparation and characterization, J. Membr. Sci., 352 (2010) 76–85.
[21] S. Mitrouli, A.J. Karabelas, A. Karanasiou, M. Kostoglou, Incipient calcium carbonate scaling of desalination membranes in narrow channels with spacers-experimental insights, J. Membr. Sci., 425 (2013) 48–57.
[22] A. Antony, J.H. Low, S. Gray, A.E. Childress, P. Le-Clech, G. Leslie, Scale formation and control in high pressure membrane water treatment systems: a review, J. Membr. Sci., 383 (2011) 1–16.
[23] D.D. Baldwin, C.E. Campbell, Short-term effects of low pH on the microfauna of an activated sludge wastewater treatment system, Water Qual. Res. J. Can., 36 (2001) 519–535.
[24] S.E. Comstock, T.H. Boyer, K.C. Graf, T.G. Townsend, Effects of landfill characteristics on leachate organic matter properties and coagulation treatability, Chemosphere, 81 (2010) 976–983.
[25] W.J. Gao, H.J. Lin, K.T. Leung, B.Q. Liao, Influence of elevated pH shocks on the performance of a submerged anaerobic membrane bioreactor, Process. Biochem., 45 (2010) 1279–1287.
[26] F. Lu, C.H. Chang, D.J. Lee, P.J. He, L.M. Shoa, A. Su, Dissolved organic matter with multi-peak fluorophores in landfill leachate, Chemosphere, 74 (2009) 575–582.
[27] S.L. Huo, B.D. Xi, H.C. Yu, H.L. Liu, Dissolved organic matter in leachate from different treatment processes, Water Environ. J., 23 (2009) 15–22.
[28] C.Y. Tang, Y.N. Kwon, J.O. Leckie, Fouling of reverse osmosis and nanofiltration membranes by humic acid-Effects of solution composition and hydrodynamic conditions, J. Membr. Sci., 290 (2007) 86–94.